

Thalamocortical dysrhythmia underpins the log-dynamics in phantom sounds

Wing Ting To^a, Jae-Jin Song^b, Anusha Mohan^d,
Dirk De Ridder^c, and Sven Vanneste^{d,*}

^a*Department of Health & Lifestyle Sciences, University of Applied Sciences,
Howest, Kortrijk, Belgium*

^b*Department of Otorhinolaryngology-Head and Neck Surgery, Seoul National University
Bundang Hospital, Seongnam, Korea*

^c*Department of Surgical Sciences, Section of Neurosurgery, Dunedin School of Medicine,
University of Otago, Dunedin, New Zealand*

^d*Global Brain Health Institute & Institute of Neuroscience, Trinity College Dublin, Dublin, Ireland*

*Corresponding author: e-mail address: sven.vanneste@tcd.ie

Abstract

Electrophysiological tinnitus research, such as EEG studies, typically investigates the irregularities in separate frequency bands. These frequency bands are coupled, such that the higher oscillation frequencies are nested (phase–amplitude coupled) on the lower frequencies, resulting in a 1/f power spectrum. The changes in the 1/f slope of the power spectrum in tinnitus patients are unexplored. Deviations from the 1/f pattern also reflect a change toward a more lattice (steeper slope) or random network (flatter slope) and relate to the amount of information in a network. In this study, we investigate the 1/f slope in the resting-state EEGs of tinnitus patients and relate these findings to proposed tinnitus mechanisms. Our data show that tinnitus is characterized by a slope that is flattened in comparison to the control group and that the tinnitus loudness percept correlates the steepness of the slope of the power spectrum in resting-state EEG signals for the left auditory cortex and left parahippocampus. The steepness of the slope is predominantly related to an increase in theta activity and its minor increase in gamma activity, suggesting that the slope is deviating toward white noise. These results should motivate further research into this hitherto elusive form of brain activity that resides behind the mask of the universal 1/f power spectrum observed across nature.

Keywords

Log-dynamics, Phantom sounds, 1/f component

1 Introduction

Electroencephalography (EEG) research has mostly focused on the synchronous activation of neuronal populations that produce rhythmic brain oscillation in specific frequency bands. These brain oscillations can be represented in frequency domains, as their power spectra contain peaks at the corresponding frequency ranges. An EEG is traditionally subdivided into different frequency bands, each with their own underlying roles: delta (1–3 Hz), theta (4–8 Hz), alpha (9–12 Hz), beta (12–30 Hz), and gamma (>30 Hz). New neuronal dynamics regimes have been explored that are characterized by arrhythmic activity (Diaz et al., 2018). Studies have been investigating broadband properties of the EEG spectrum and have identified a predominant “1/f” component that falls off with increasing frequency following a power-law function: $P \propto 1/f^\beta$ where P is power, f is frequency, and β is the power-law or spectral exponent typically in the range between 0 and 3 (He, 2014). This power-law distribution of the power spectrum is also named “scale-free” or “fractal” dynamics and is commonly referred to as “1/f noise” (Allegrini et al., 2009; Buzsaki and Mizuseki, 2014; He et al., 2010). Depending on the spectral exponent pink, brown and white noise have been described (Keshner, 1982). Pink noise is characterized by a power-law exponent around 1 (Leong et al., 2018), brown noise around 2 (Freeman and Zhai, 2009) and black noise larger than 2 (Freeman and Zhai, 2009). In white noise all frequencies typically have equal power, meaning that the power-law exponent is 0, or the spectral density is flat (Keshner, 1982). White noise represents a maximum of informational entropy (Shannon, 1948), in other words a lack of information content, as there is no structure embedded in the noise. All frequencies are independent of each other (Shannon, 1948), in contrast to structured, i.e., colored noise (Kosko, 2006).

For a long time, brain activity that contained in the “1/f” slope has been deemed unimportant, i.e., noise, and was often removed from the analysis in order to emphasize brain oscillations (He, 2014). Increasing evidence however suggests that arrhythmic brain activity contributes to brain functioning and that the 1/f slope can vary in significant ways (El Boustani et al., 2009; Freeman and Zhai, 2009; Podvalny et al., 2015; Voytek and Knight, 2015). Several brain studies have demonstrated that for healthy subjects the entropy of neural time series is characterized by roughly 1/f or pink noise and that signals show pink noise behavior when excitatory and inhibitory influences are balanced (Dehghani et al., 2010; El Boustani et al., 2009; He, 2011; He et al., 2010; Milstein et al., 2009; Radulescu and Mujica-Parodi, 2014). Studies demonstrate that this 1/f-like power spectra shifts toward a white ($1/f^0$) noise in several brain disorders including schizophrenia (Radulescu et al., 2012; Slezin et al., 2007), anxiety (Tolkunov et al., 2010), autism (Lai et al., 2010; Weinger et al., 2014), fibromyalgia (Gonzalez-Villar et al., 2017), and Alzheimer’s disease (Protzner et al., 2010; Vysata et al., 2014). From an information theory point of view this suggests that these disorders are related to a less information processing.

Instead of investigating irregularities in the different frequency bands, disorders can be approached by considering the entire power spectrum as a unified statistical

representation of the signal, reflected by a change in the 1/f slope of the power spectrum. This new approach has not yet been investigated for tinnitus. Tinnitus is considered an auditory phantom perception and can present as a noise or a tone, or complex sound percept in the absence of any objective corresponding physical sound source (Jastreboff, 1990). The lack of auditory input results in a lack of information the auditory system can use to reduce auditory uncertainty, inherently present in the environment (De Ridder et al., 2014a).

Thalamocortical dysrhythmia (TCD) in the left auditory cortex and the left hippocampus has been associated with deafferentation related chronic tinnitus (De Ridder et al., 2015; Llinas et al., 2005, 1999; Vanneste et al., 2018). The original description of thalamocortical dysrhythmia proposes that normal resting-state alpha activity (8–12 Hz) slows down to theta (4–8 Hz) activity in states of deprived input. This theta activity is then associated with an increase in surrounding beta/gamma (25–50 Hz) activity, which results in persistent cross-frequency coupling between theta and gamma activity (Llinas et al., 1999, 2005; Vanneste et al., 2018). The underlying idea is that deprivation leads to a thalamocortical column-specific decrease in information processing, which permits slowing down of resting-state thalamocortical activity from alpha to theta, as less information needs to be processed (Borst and Theunissen, 1999). Decreased input also results in a reduction of GABA_A-mediated lateral inhibition, inducing gamma (>30 Hz) band activity surrounding the deafferented thalamocortical columns (Llinas et al., 2005). This gamma band activity surrounding theta activity is known as the edge effect (Llinas et al., 1999, 2005).

In the past, tinnitus researchers have investigated the irregularities in the many frequency bands separately. However, the overall cross-frequency coupling between the different frequency bands, reflected in changes in the 1/f slope of the power spectrum (Voytek et al., 2015) in tinnitus patients is unexplored. In this study, we investigate the changes in the 1/f slope of the power spectrum and discuss these findings in the light of the proposed tinnitus mechanisms. As tinnitus is a simple phantom percept similar to phantom pain (De Ridder et al., 2011a; Hullfish et al., 2019; Mohan and Vanneste, 2017; Vanneste et al., 2013) with comorbidities such as depression and anxiety, we expect spectra shifts toward a white noise based on auditory input deprivation. It has further been suggested that in a 1/f relationship, perturbations that occur at slow frequencies (i.e., theta) cause a cascade of energy disposition at beta and gamma frequencies as widespread slow oscillations modulate faster local events (Buzsaki and Draguhn, 2004). We hypothesize that theta might influence the 1/f structure slope in the auditory cortex and hippocampus for tinnitus patients, as these two structures are critically involved in a Bayesian explanation for the generation of tinnitus (De Ridder et al., 2014a). The lack of auditory input will be reflected from an information theory point of view by a flattening of the spectral exponent slope. Neurophysiologically this would be the result of the thalamocortical dysrhythmia model of auditory deprivation. The goal of this study was to verify whether information theoretical approaches to tinnitus and neurophysiological data are consistent.

2 Methods and materials

2.1 Participants

One-hundred and twenty patients with chronic tinnitus were included after exclusion of individuals with pulsatile tinnitus, Meniere's disease, otosclerosis, chronic headache, neurological disorders (i.e., brain tumors), and individuals being treated for mental disorders in order to increase the sample homogeneity.

One-hundred and twenty healthy non-tinnitus controls participated, who were age-matched and gender matched, as the 1/f slope changes (flattens) which age ([Voytek et al., 2015](#)). None of these subjects were known to suffer from tinnitus, were matched for hearing loss at a group level. Exclusion criteria included: known psychiatric or neurological illness, psychiatric history or drug/alcohol abuse, history of head injury (with loss of consciousness) or seizures, headache, or physical disability. For these healthy controls hearing assessment was also performed.

All participating patients were screened for the severity of hearing loss using the British Society of Audiology pure tone audiometry procedures (Electronics Orbiter 922 Version 2 in a soundproof audiometric booth using TDH-39 headphone as transducer) at 0.125, 0.25, 0.5, 1, 2, 3, 4, 6, and 8 kHz ([British Society of Audiology, 2008](#)). See [Fig. 1](#) for a comparison between the control group and the tinnitus group.

See [Table 1](#) for a comparison between the control group and the tinnitus group for demographics.

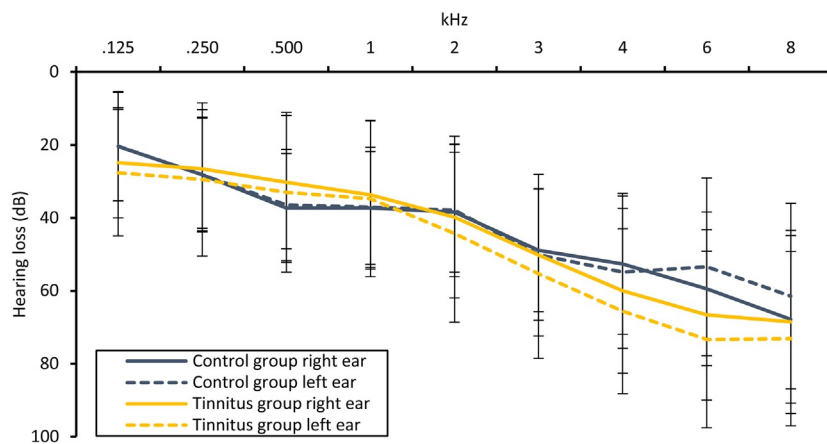


FIG. 1

Using a median split the tinnitus group was divided into two subgroups, one without clinical hearing loss, and one with severe hearing loss (top left and top right figures). The subgroup with severe hearing loss perceived tinnitus significantly louder (bottom left) and experienced tinnitus more distressing (bottom right) than the subgroup without clinical hearing loss.

Table 1 Demographics.

	Control group	Tinnitus group
Age	$M=49.05, Sd=11.21$	$M=48.32, Sd=11.21$
Gender	♀: 78 ♂: 42	♀: 64 ♂: 56
Tinnitus-related distress	–	$M=42.15, Sd=9.57$
Tinnitus type	–	Pure tone: 66 Narrow band noise: 54
Tinnitus location	–	Left ear: 34 Right ear: 29 Bilateral: 57

2.2 Tinnitus measures

Numeric rating scale (NRS). Tinnitus loudness using a numeric rating scale between 0 and 10 was used to evaluate the subjectively perceived tinnitus loudness based on the question: “How loud is your tinnitus?” (0=no tinnitus and 10=as loud as imaginable).

Tinnitus Questionnaire (TQ). Tinnitus-related distress was assessed using the Tinnitus Questionnaire (TQ). This scale is comprised of 52 items and is a well-established measure for the assessment of a broad spectrum of tinnitus-related psychological complaints. The global TQ score can be computed to measure the general level of psychological and psychosomatic distress. A 3-point scale is given for all items, ranging from “true” (2 points) to “partly true” (1 point) and “not true” (0 points). The total score (from 0 to 84) was computed according to standard criteria published in previous work (Hiller et al., 1994; Hiller and Goebel, 1992; Meeus et al., 2007).

2.3 EEG data collection and processing

EEG recordings were obtained in a fully lighted room with each participant sitting upright on a comfortable chair. The actual recording lasted approximately 5 min. The EEG was sampled using Mitsar-201 amplifiers (NovaTech <http://www.novatecheeg.com/>) with 19 electrodes placed according to the standard 10–20 International placement. Impedances were checked to remain below 5 kΩ. Data were collected while the subject’s eyes were closed (sampling rate = 500 Hz, band passed 0.15–200 Hz). Off-line data were band-pass filtered in the range 2–43 Hz, resampled to 128 Hz and subsequently transposed into Eureka! Software (Congedo, 2002). The data were then plotted and carefully inspected for manual artifact rejection. All episodic artifacts including eye movements, teeth clenching, body movement, or electrocardiac artifact were removed from the stream of the EEG. Fourier cross-spectral matrices were computed for frequency from 2 to 43 Hz for epochs of 2 s.

Standardized low-resolution brain electromagnetic tomography (sLORETA; Pascual-Marqui, 2002) was used to estimate the intracerebral electrical sources that

generated the recorded activity (at sensory level). As a standard procedure, a common average reference transformation (Pascual-Marqui, 2002) is performed before applying the sLORETA algorithm. sLORETA computes electric neuronal activity as current density (A/mm^2) without assuming a predefined number of active sources. The solution space used in this study and associated leadfield matrix are those implemented in the LORETA-Key software (freely available at <http://www.uzh.ch/keyinst/loreta.htm>). The sLORETA-key anatomical template divides and labels the neocortical (including hippocampus and anterior cingulated cortex) MNI-152 volume in 6239 voxels of dimension 5 mm^3 , based on probabilities returned by the Demon Atlas (Lancaster et al., 2000). The co-registration makes use of the correct translation from the MNI-152 space into the Talairach and Tournoux space (Brett et al., 2002). The log-transformed electric current density was calculated for left auditory cortex, left parahippocampus as regions of interests. The selection of these regions of interest was based on our hypothesis as introduced in the introduction (a priori).

2.4 Current density

The log-transformed electric current density was calculated for left auditory cortex and left parahippocampus for the gamma frequency bands (30.5–43 Hz). As the voxel-size of each region of interest has the dimension 5 mm^3 , we only used this voxel.

2.5 Cross-frequency coupling

Theta–gamma coupling (e.g., by nesting) is proposed to be an effective manner of communication between cortically distant areas (Canolty et al., 2006). To verify whether this theta–gamma nesting is present, it was calculated for, left auditory cortex, and the left parahippocampus cortex using phase–amplitude cross-frequency coupling. Phase–amplitude was chosen over power–power cross-frequency coupling as the former has been shown to reflect a physiological mechanism for effective communication in the human brain (Canolty et al., 2006). Nesting was computed by first obtaining the time series for the x, y, and z components of the sLORETA current for the voxel of each ROI. These are the time series of the electrical current in the three orthogonal directions in space. Next, these were filtered in the theta (4–7.5 Hz) and gamma (30.5–43 Hz) frequency band-pass regions. In each frequency band and for each ROI, a principal component analysis for the overall x, y, z component was computed and the first component was retained for the theta and gamma bands. The Hilbert transform was then computed on the gamma component and the signal envelope retained. Finally, the Pearson correlation between the theta component and the envelope of the gamma envelope was computed for each individual.

2.6 Data analysis

Power spectrum (PS) of biological time series (of an electroencephalogram recording, for instance) often shows a relationship of decreasing power as a function of frequency (f) according to the general equation: $PS(f) = \psi \times f^\alpha$ (Norena et al., 2010).

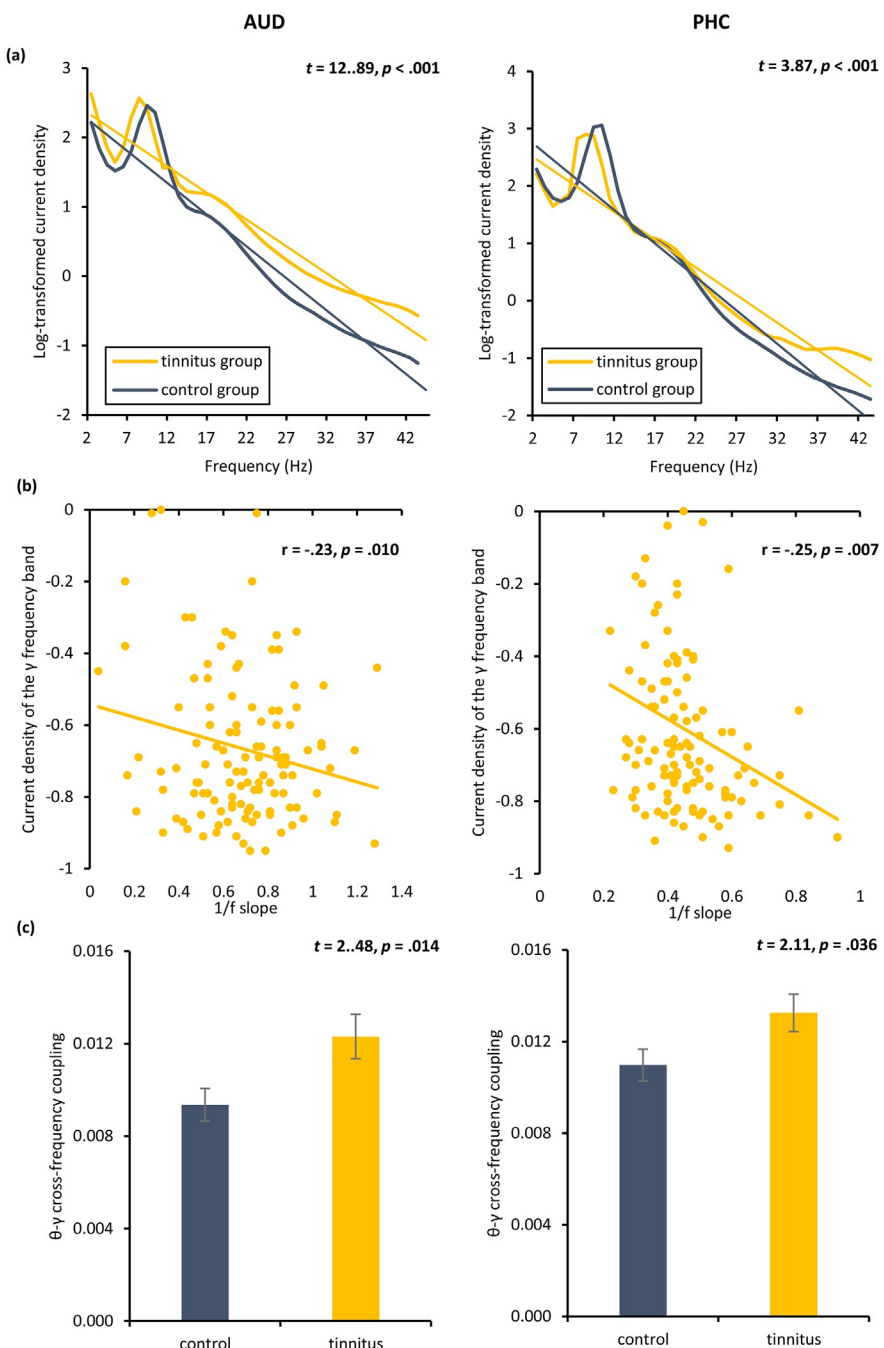
The exponent α , therefore, represents the rate at which the power spectrum decreases as a function of frequency, and gives an estimate about the length (or “distance”) of the linear correlations within the time series in question. In other words, the slope of the power spectrum provides an index of “temporal memory effects” in the time series (Buzsaki, 2006). A white noise, for instance, has no correlation over time (its autocorrelation is represented by a Dirac function) and there is no relationship between frequency bands. As a consequence, the power spectrum of white noise is flat. A Brownian noise (or random walk noise), on the other hand, presents correlations over (short) time. In a “random walk” pattern, the position of a particle at time $t+1$ will depend on its position at time t . Correlations in the time domain, then, have their counterpart in the frequency domain: the power spectra of white noise and Brownian noise are proportional to f^α , with $\alpha=0$ and 2, respectively. What is called “pink noise” falls between white noise and Brownian noise with $\alpha=1$. It is noteworthy that it has been suggested that the power spectrum of spontaneous neural signals follow the general rule f^α , with α close to 1 (Buzsaki, 2006). The exponent α was obtained from a linear regression between the PS and frequency (f), as follows: $\log(PS)=\alpha \times \log(f)+\beta$. The exponent α was calculated for each artifact-free epoch of silence, for values in the range between $f=1$ and $f=43$ Hz. The mean average on all individual β_1 epochs (i.e., steepness of the slope) was calculated for the tinnitus group and the healthy controls. We compared the steepness of the slope for the two groups for both regions of interest using a regression analysis and by looking at the interaction between the steepness of the slope and group (i.e., t -test). For the tinnitus group a Pearson correlation was calculated for the link between the steepness of the slope and the log-transformed electric current density at both theta and gamma frequency for both left auditory cortex and left parahippocampus. For the cross-frequency coupling, an independent t -test was calculated to compare the theta–gamma coupling between the control and tinnitus group for both left auditory cortex and left parahippocampus, respectively.

A Pearson correlation was calculated for the association between the tinnitus loudness and the steepness of the slope for both left auditory cortex and left parahippocampus, respectively.

A Pearson correlation was calculated for the relationship between the tinnitus loudness and the log-transformed electric current density with the theta and gamma frequency bands for both left auditory cortex and left parahippocampus, respectively. Similar analyses were calculated for the average hearing loss with the slope and the log-transformed electric current density, respectively.

3 Results

A comparison between the average steepness of the slope between tinnitus patients and healthy controls revealed a significant difference for both the left auditory cortex ($t=12.89$, $p<0.001$) and left parahippocampus ($t=3.87$, $p<0.001$). This finding suggests that the average slope was significantly steeper for the healthy controls than for the tinnitus subjects (see Fig. 2A). This effect is mainly driven by a slowing down

**FIG. 2**

See figure legend on opposite page.

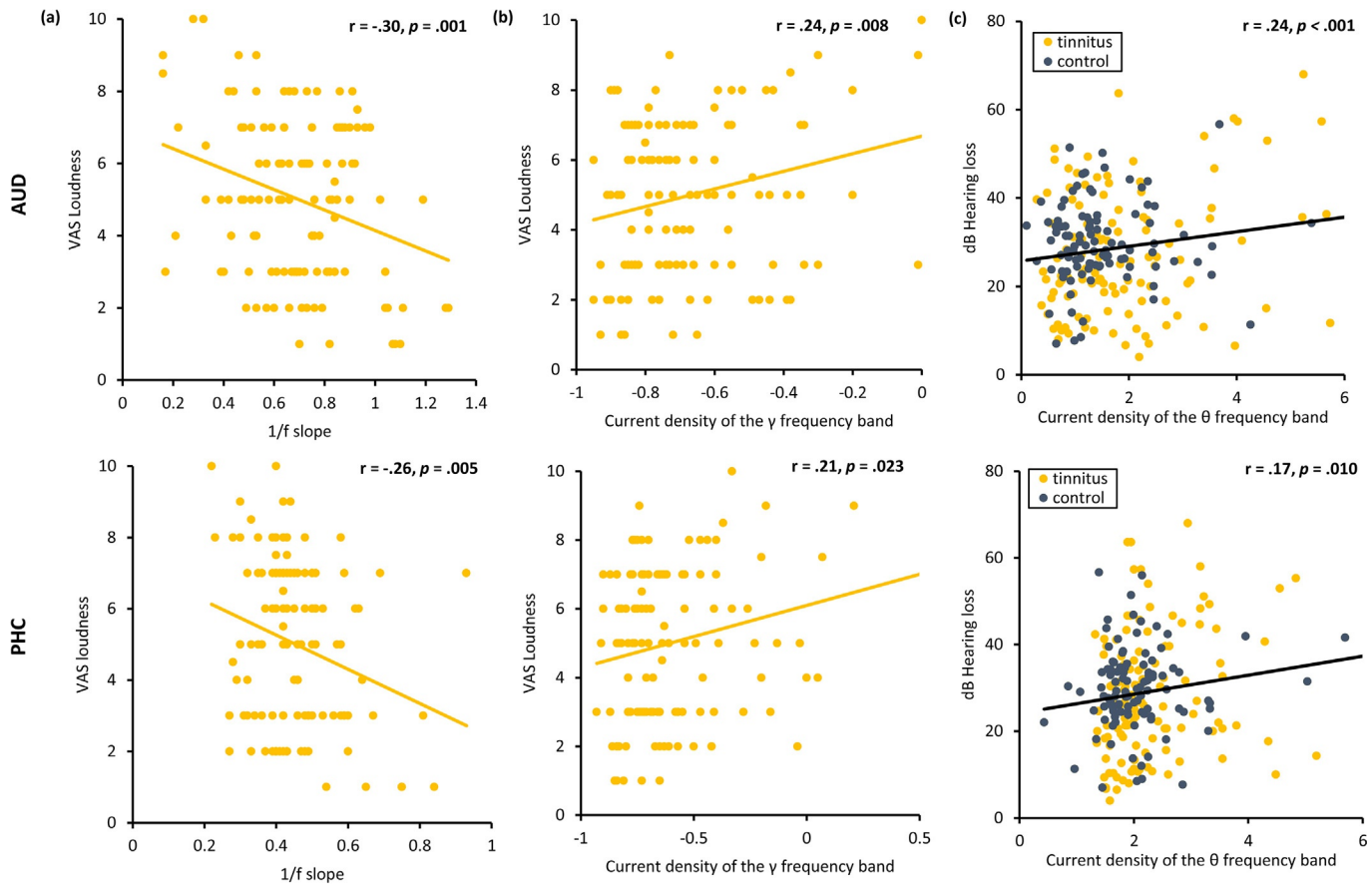
of the alpha oscillations that is associated with an increase in the gamma frequency band. A correlation between the steepness of the slope and the log-transformed current density for the gamma frequency band revealed a significant effect for both the left auditory cortex ($r = -0.23, p = 0.010$) and the left parahippocampus ($r = -0.25, p = 0.007$) subjects (see Fig. 2B). This effect revealed a negative association between the steepness of the slope and the log-transformed current density for the gamma frequency band, indicating the flatter the slope the more current density is identified within left auditory cortex and the left parahippocampus. No significant correlation was obtained between the steepness of the slope and the log-transformed current density in the theta frequency band for the left auditory cortex and the left parahippocampus. In addition, we applied a theta–gamma cross-frequency coupling revealing that for both the left auditory cortex ($t = 2.48, p = 0.014$) and left parahippocampus ($t = 2.11, p = 0.036$) increased theta–gamma cross-frequency coupling was identified for the tinnitus group in comparison to the control group (see Fig. 2C).

A significant negative correlation was revealed between the individual steepness of the slope and the tinnitus loudness in the left auditory cortex ($r = -0.30, p = 0.001$) and the left parahippocampus ($r = -0.26, p = 0.005$) (see Fig. 3A). These changes are mainly driven by a more pronounced gamma increase. Indeed, a significant correlation was obtained between the loudness and the log-transformed current density in the gamma frequency band for the left auditory cortex ($r = 0.24, p = 0.008$) and the left parahippocampus ($r = 0.21, p = 0.023$) suggesting that the higher the current density, the louder patients perceived their tinnitus, or vice versa (see Fig. 3B). No significant correlation was obtained between the loudness and the log-transformed current density in the theta frequency band for the left auditory cortex and the left parahippocampus.

No significant correlation was found between the individual steepness of the slope and the mean hearing loss for the left auditory cortex and the left parahippocampus. However, a significant positive correlation was identified between the mean hearing loss and the log-transformed current density in the theta frequency band for the left auditory cortex ($r = 0.24, p < 0.001$) and the left parahippocampus ($r = 0.17, p = 0.010$) indicating that more hearing loss is associated with higher current density

FIG. 2

(A) A comparison between the average steepness of the slope between tinnitus subjects and control group demonstrates the slope becomes flatter in tinnitus patients in comparison to healthy controls for both the left auditory cortex and left parahippocampus. The slope becomes less steep in both brain areas. (B) Pearson correlations between the individual steepness of the slope and tinnitus loudness for the tinnitus group. The steepness of the slope correlates negatively with the tinnitus loudness for both the auditory cortex and parahippocampus. (C) The current density for the gamma frequency band for both the left auditory cortex and left parahippocampus correlates positively with the tinnitus loudness. (D) A negative correlation was obtained between the steepness of the slope and the current density for the gamma frequency band for both the left auditory cortex and left parahippocampus in tinnitus patients.

**FIG. 3**

A cross-frequency coupling between the theta and gamma for both the left auditory cortex and left parahippocampus is significantly increased in the tinnitus group in comparison to the control group.

within the theta frequency band (see Fig. 3C). No significant correlation was obtained between the mean hearing loss and the log-transformed current density in the gamma frequency band for the left auditory cortex and the left parahippocampus.

4 Discussion

This study approached tinnitus as a shift in global frequency band correlation instead of investigating abnormalities in the many frequency bands in tinnitus-related brain areas. In line with previous research in other pathologies, in patients with tinnitus a flatter 1/f slope, i.e., a whitening of the power spectrum was identified compared to controls, in keeping with an information theoretical approach to tinnitus.

This study showed a relation between the subjectively perceived tinnitus loudness and the steepness of the slope of the power spectrum in resting-state EEG signals for the left auditory cortex and left parahippocampus. These brain areas have been implicated in tinnitus (De Ridder et al., 2014b; Langguth et al., 2012; Vanneste et al., 2011; Vanneste and De Ridder, 2012) and were characterized by a slope that is flattened in comparison to the control group. This seems to be predominantly related to an increase in gamma frequency activity. This suggests a shift-to-randomness of brain oscillations, from a pink noise to white noise structure, in the tinnitus brain. This shift is not unique to tinnitus as this has also been observed in schizophrenia (Radulescu et al., 2012), anxiety (Tolkunov et al., 2010), autism (Lai et al., 2010), and Alzheimer's disease (Vysata et al., 2014). Our finding fits with the idea that log-dynamics are associated with risk for neurological and psychiatric illnesses that are deregulatory in nature (Tolkunov et al., 2010). The question remains why a shift from pink to a more random white noise structure is related to different pathologies. It has been suggested that pink noise ($1/f^1$) is the optimal transition between order and disorder, an optimal "sweet-spot", which permits both flexibility and stability (Hellyer et al., 2014; Van Orden et al., 2005), as well as being optimal for signal transmission in a noisy environment. Indeed, 1/f signals themselves can be encoded and transmitted by sensory neurons with higher efficiency (Yu et al., 2005). This could be related to the fact that 1/f background noise enhances the sensitivity of neurons to subthreshold signals better than white noise (Nozaki et al., 1999; Soma et al., 2003). Thus, in tinnitus patients the shift to more white noise may imply less efficacious signal transmission, especially in the tinnitus-related network.

A negative correlation was found between the subjectively perceived tinnitus loudness and the steepness of the slope for the left auditory cortex and the left parahippocampus. Our findings indicate that the louder the patients perceive their tinnitus, the less steep the slope in the left auditory cortex and the left parahippocampus. The steepness of the slope is predominantly related to an increase in gamma activity, suggesting that the slope is normalizing toward white noise. Based on the thalamocortical dysrhythmia model, the dominant resting-state alpha rhythm decreases to theta band activity (De Ridder et al., 2015; Llinas et al., 1999, 2005;

Vanneste et al., 2018). Increased theta and gamma activity in the left auditory cortex and left parahippocampus, that is coupled, has been linked to deafferentation (Vanneste et al., 2019; Vanneste and De Ridder, 2016). It was proposed that theta reflects the negative symptoms (hearing loss, hypoesthesia, ...) and gamma the positive symptoms (i.e., tinnitus) in diseases characterized by TCD (Llinas et al., 2005; Llinas and Steriade, 2006), which is confirmed by this study. Thus, the negative symptoms (i.e., hearing loss) are proposed to be linked to less information processing and therefore slowed alpha activity, as if the deafferented thalamocortical columns are “as asleep” (Llinas et al., 2005). It has been proposed that this theta could then act as a long-range carrier wave (Freeman, 2003) on which the tinnitus information can be nested by means of gamma oscillatory activity (De Ridder et al., 2014b, 2015). This fits our data, which demonstrated a correlation between the slope and the tinnitus loudness, and the increase of coupled gamma–theta wave activity in the tinnitus patients.

Overall, our findings link an information theoretical and neurophysiological approach to explain tinnitus. Both critically depend on the concept that missing auditory information is essential in the generation of tinnitus. The tinnitus is likely linked to a difference in information transmission (due to auditory deprivation) thereby flattening the slope. Neurophysiologically this is based on a slowing down of alpha activity to theta in the auditory cortex or parahippocampus in tinnitus associated with increased gamma activity (De Ridder et al., 2014a, 2015).

References

- Allegrini, P., Menicucci, D., Bedini, R., Fronzoni, L., Gemignani, A., Grigolini, P., ... Paradisi, P., 2009. Spontaneous brain activity as a source of ideal 1/f noise. *Phys. Rev. E Stat. Nonlin. Soft Matter Phys.* 80 (6 Pt 1), 061914. Retrieved from <http://www.ncbi.nlm.nih.gov/pubmed/20365197>.
- Borst, A., Theunissen, F.E., 1999. Information theory and neural coding. *Nat. Neurosci.* 2 (11), 947–957. <https://doi.org/10.1038/14731>.
- Brett, M., Johnsrude, I.S., Owen, A.M., 2002. The problem of functional localization in the human brain. *Nat. Rev. Neurosci.* 3 (3), 243–249. <https://doi.org/10.1038/nrn756>.
- British Society of Audiology, 2008. Recommended Procedure: Pure Tone Air and Bone Conduction Threshold Audiometry With and Without Masking and Determination of Uncomfortable Loudness Levels. British Society of Audiology.
- Buzsaki, G., 2006. *Rhythms of the Brain*. New York, Oxford.
- Buzsaki, G., Draguhn, A., 2004. Neuronal oscillations in cortical networks. *Science* 304 (5679), 1926–1929. <https://doi.org/10.1126/science.1099745>. 304/5679/1926 [pii].
- Buzsaki, G., Mizuseki, K., 2014. The log-dynamic brain: how skewed distributions affect network operations. *Nat. Rev. Neurosci.* 15 (4), 264–278. <https://doi.org/10.1038/nrn3687>.
- Canolty, R.T., Edwards, E., Dalal, S.S., Soltani, M., Nagarajan, S.S., Kirsch, H.E., ... Knight, R.T., 2006. High gamma power is phase-locked to theta oscillations in human neocortex. *Science* 313 (5793), 1626–1628. <https://doi.org/10.1126/science.1128115>. 313/5793/1626 [pii].

- Congedo, M., 2002. EureKa! (Version 3.0) [Computer Software]. NovaTech EEG Inc. Freeware, Knoxville, TN. available at www.NovaTechEEG.
- De Ridder, D., Elgoyhen, A.B., Romo, R., Langguth, B., 2011a. Phantom percepts: tinnitus and pain as persisting aversive memory networks. *Proc. Natl. Acad. Sci. U. S. A.* 108 (20), 8075–8080. <https://doi.org/10.1073/pnas.1018466108>. 1018466108 [pii].
- De Ridder, D., Vanneste, S., Freeman, W., 2014a. The Bayesian brain: phantom percepts resolve sensory uncertainty. *Neurosci. Biobehav. Rev.* 44C, 4–15. <https://doi.org/10.1016/j.neubiorev.2012.04.001>.
- De Ridder, D., Vanneste, S., Weisz, N., Londero, A., Schlee, W., Elgoyhen, A.B., Langguth, B., 2014b. An integrative model of auditory phantom perception: tinnitus as a unified percept of interacting separable subnetworks. *Neurosci. Biobehav. Rev.* 44, 16–32. <https://doi.org/10.1016/j.neubiorev.2013.03.021>.
- De Ridder, D., Vanneste, S., Langguth, B., Llinas, R., 2015. Thalamocortical dysrhythmia: a theoretical update in tinnitus. *Front. Neurol.* 6, 124. <https://doi.org/10.3389/fneur.2015.00124>.
- Dehghani, N., Bedard, C., Cash, S.S., Halgren, E., Destexhe, A., 2010. Comparative power spectral analysis of simultaneous electroencephalographic and magnetoencephalographic recordings in humans suggests non-resistive extracellular media. *J. Comput. Neurosci.* 29 (3), 405–421. <https://doi.org/10.1007/s10827-010-0263-2>.
- Diaz, J., Bassi, A., Coolen, A., Vivaldi, E.A., Letelier, J.C., 2018. Envelope analysis links oscillatory and arrhythmic EEG activities to two types of neuronal synchronization. *Neuroimage* 172, 575–585. <https://doi.org/10.1016/j.neuroimage.2018.01.063>.
- El Boustani, S., Marre, O., Behuret, S., Baudot, P., Yger, P., Bal, T., ... Fregnac, Y., 2009. Network-state modulation of power-law frequency-scaling in visual cortical neurons. *PLoS Comput. Biol.* 5 (9), e1000519. <https://doi.org/10.1371/journal.pcbi.1000519>.
- Freeman, W.J., 2003. The wave packet: an action potential for the 21st century. *J. Integr. Neurosci.* 2 (1), 3–30. Retrieved from http://www.ncbi.nlm.nih.gov/entrez/query.fcgi?cmd=Retrieve&db=PubMed&dopt=Citation&list_uids=15011274.
- Freeman, W.J., Zhai, J., 2009. Simulated power spectral density (PSD) of background electrocorticogram (ECOG). *Cogn. Neurodyn.* 3 (1), 97–103. <https://doi.org/10.1007/s11571-008-9064-y>.
- Gonzalez-Villar, A.J., Samartin-Veiga, N., Arias, M., Carrillo-de-la-Pena, M.T., 2017. Increased neural noise and impaired brain synchronization in fibromyalgia patients during cognitive interference. *Sci. Rep.* 7 (1), 5841. <https://doi.org/10.1038/s41598-017-06103-4>.
- He, B.J., 2011. Scale-free properties of the functional magnetic resonance imaging signal during rest and task. *J. Neurosci.* 31 (39), 13786–13795. <https://doi.org/10.1523/JNEUROSCI.2111-11.2011>.
- He, B.J., 2014. Scale-free brain activity: past, present, and future. *Trends Cogn. Sci.* 18 (9), 480–487. <https://doi.org/10.1016/j.tics.2014.04.003>.
- He, B.J., Zempel, J.M., Snyder, A.Z., Raichle, M.E., 2010. The temporal structures and functional significance of scale-free brain activity. *Neuron* 66 (3), 353–369. <https://doi.org/10.1016/j.neuron.2010.04.020>. S0896-6273(10)00291-6 [pii].
- Hellyer, P.J., Shanahan, M., Scott, G., Wise, R.J., Sharp, D.J., Leech, R., 2014. The control of global brain dynamics: opposing actions of frontoparietal control and default mode networks on attention. *J. Neurosci.* 34 (2), 451–461. <https://doi.org/10.1523/JNEUROSCI.1853-13.2014>.

- Hiller, W., Goebel, G., 1992. A psychometric study of complaints in chronic tinnitus. *J. Psychosom. Res.* 36 (4), 337–348. Retrieved from http://www.ncbi.nlm.nih.gov/entrez/query.fcgi?cmd=Retrieve&db=PubMed&dopt=Citation&list_uids=1593509.
- Hiller, W., Goebel, G., Rief, W., 1994. Reliability of self-rated tinnitus distress and association with psychological symptom patterns. *Br. J. Clin. Psychol.* 33 (Pt 2), 231–239. Retrieved from http://www.ncbi.nlm.nih.gov/entrez/query.fcgi?cmd=Retrieve&db=PubMed&dopt=Citation&list_uids=8038742.
- Hullfish, J., Sedley, W., Vanneste, S., 2019. Prediction and perception: insights for (and from) tinnitus. *Neurosci. Biobehav. Rev.* 102, 1–12. <https://doi.org/10.1016/j.neubiorev.2019.04.008>.
- Jastreboff, P.J., 1990. Phantom auditory perception (tinnitus): mechanisms of generation and perception. *Neurosci. Res.* 8 (4), 221–254. Retrieved from http://www.ncbi.nlm.nih.gov/entrez/query.fcgi?cmd=Retrieve&db=PubMed&dopt=Citation&list_uids=2175858.
- Keshner, M.S., 1982. 1/f noise. *Proc. IEEE* 70 (3), 212–218.
- Kosko, B., 2006. Noise. Penguin, New York.
- Lai, M.C., Lombardo, M.V., Chakrabarti, B., Sadek, S.A., Pasco, G., Wheelwright, S.J., ... Suckling, J., 2010. A shift to randomness of brain oscillations in people with autism. *Biol. Psychiatry* 68 (12), 1092–1099. <https://doi.org/10.1016/j.biopsych.2010.06.027>.
- Lancaster, J.L., Woldorff, M.G., Parsons, L.M., Liotti, M., Freitas, C.S., Rainey, L., ... Fox, P.T., 2000. Automated Talairach atlas labels for functional brain mapping. *Hum. Brain Mapp.* 10 (3), 120–131. Retrieved from <https://www.ncbi.nlm.nih.gov/pubmed/10912591>.
- Langguth, B., Schecklmann, M., Lehner, A., Landgrebe, M., Poepll, T.B., Kreuzer, P.M., ... De Ridder, D., 2012. Neuroimaging and neuromodulation: complementary approaches for identifying the neuronal correlates of tinnitus. *Front Syst Neurosci* 6, 15. <https://doi.org/10.3389/fnsys.2012.00015>.
- Leong, S.L., De Ridder, D., Vanneste, S., Sutherland, W., Ross, S., Manning, P., 2018. High definition transcranial pink noise stimulation of anterior cingulate cortex on food craving: an explorative study. *Appetite* 120, 673–678. <https://doi.org/10.1016/j.appet.2017.10.034>.
- Llinas, R.R., Steriade, M., 2006. Bursting of thalamic neurons and states of vigilance. *J. Neurophysiol.* 95 (6), 3297–3308. <https://doi.org/10.1152/jn.00166.2006>.
- Llinas, R.R., Ribary, U., Jeanmonod, D., Kronberg, E., Mitra, P.P., 1999. Thalamocortical dysrhythmia: a neurological and neuropsychiatric syndrome characterized by magnetoencephalography. *Proc. Natl. Acad. Sci. U. S. A.* 96 (26), 15222–15227. Retrieved from http://www.ncbi.nlm.nih.gov/entrez/query.fcgi?cmd=Retrieve&db=PubMed&dopt=Citation&list_uids=10611366.
- Llinas, R., Urbano, F.J., Leznik, E., Ramirez, R.R., van Marle, H.J., 2005. Rhythmic and dysrhythmic thalamocortical dynamics: GABA systems and the edge effect. *Trends Neurosci.* 28 (6), 325–333. Retrieved from http://www.ncbi.nlm.nih.gov/entrez/query.fcgi?cmd=Retrieve&db=PubMed&dopt=Citation&list_uids=15927689.
- Meeus, O., Blaivie, C., Van de Heyning, P., 2007. Validation of the Dutch and the French version of the tinnitus questionnaire. *B-ENT* 3 (Suppl 7), 11–17. Retrieved from http://www.ncbi.nlm.nih.gov/entrez/query.fcgi?cmd=Retrieve&db=PubMed&dopt=Citation&list_uids=18228680.
- Milstein, J., Mormann, F., Fried, I., Koch, C., 2009. Neuronal shot noise and Brownian 1/f² behavior in the local field potential. *PLoS One* 4 (2), e4338. <https://doi.org/10.1371/journal.pone.0004338>.

- Mohan, A., Vanneste, S., 2017. Adaptive and maladaptive neural compensatory consequences of sensory deprivation—from a phantom percept perspective. *Prog. Neurobiol.* 153, 1–17. <https://doi.org/10.1016/j.pneurobio.2017.03.010>.
- Norena, A.J., Moffat, G., Blanc, J.L., Pezard, L., Cazals, Y., 2010. Neural changes in the auditory cortex of awake Guinea pigs after two tinnitus inducers: salicylate and acoustic trauma. *Neuroscience* 166 (4), 1194–1209. <https://doi.org/10.1016/j.neuroscience.2009.12.063>. S0306-4522(09)02151-4 [pii].
- Nozaki, D., Collins, J.J., Yamamoto, Y., 1999. Mechanism of stochastic resonance enhancement in neuronal models driven by 1/f noise. *Phys. Rev. E Stat. Phys. Plasmas Fluids Relat. Interdiscip. Topics* 60 (4 Pt B), 4637–4644. Retrieved from <http://www.ncbi.nlm.nih.gov/pubmed/11970325>.
- Pascual-Marqui, R.D., 2002. Standardized low-resolution brain electromagnetic tomography (sLORETA): technical details. *Methods Find. Exp. Clin. Pharmacol.* 24 (Suppl D), 5–12. Retrieved from http://www.ncbi.nlm.nih.gov/entrez/query.fcgi?cmd=Retrieve&db=PubMed&dopt=Citation&list_uids=12575463.
- Podvalny, E., Noy, N., Harel, M., Bickel, S., Chechik, G., Schroeder, C.E., ... Malach, R., 2015. A unifying principle underlying the extracellular field potential spectral responses in the human cortex. *J. Neurophysiol.* 114 (1), 505–519. <https://doi.org/10.1152/jn.00943.2014>.
- Protzner, A.B., Valiante, T.A., Kovacevic, N., McCormick, C., McAndrews, M.P., 2010. Hippocampal signal complexity in mesial temporal lobe epilepsy: a noisy brain is a healthy brain. *Arch. Ital. Biol.* 148 (3), 289–297. Retrieved from <http://www.ncbi.nlm.nih.gov/pubmed/21175015>.
- Radulescu, A., Mujica-Parodi, L.R., 2014. Network connectivity modulates power spectrum scale invariance. *Neuroimage* 90, 436–448. <https://doi.org/10.1016/j.neuroimage.2013.12.001>.
- Radulescu, A.R., Rubin, D., Strey, H.H., Mujica-Parodi, L.R., 2012. Power spectrum scale invariance identifies prefrontal dysregulation in paranoid schizophrenia. *Hum. Brain Mapp.* 33 (7), 1582–1593. <https://doi.org/10.1002/hbm.21309>.
- Shannon, C.E., 1948. A mathematical theory of communication. *Bell Syst. Tech. J.* 27 (379–423), 623–656.
- Slezin, V.B., Korsakova, E.A., Dytjatkovsky, M.A., Schultz, E.A., Arystova, T.A., Siivola, J.R., 2007. Multifractal analysis as an aid in the diagnostics of mental disorders. *Nord. J. Psychiatry* 61 (5), 339–342. <https://doi.org/10.1080/08039480701643175>.
- Soma, R., Nozaki, D., Kwak, S., Yamamoto, Y., 2003. 1/f noise outperforms white noise in sensitizing baroreflex function in the human brain. *Phys. Rev. Lett.* 91 (7), 078101. Retrieved from <http://www.ncbi.nlm.nih.gov/pubmed/12935054>.
- Tolkunov, D., Rubin, D., Mujica-Parodi, L., 2010. Power spectrum scale invariance quantifies limbic dysregulation in trait anxious adults using fMRI: adapting methods optimized for characterizing autonomic dysregulation to neural dynamic time series. *Neuroimage* 50 (1), 72–80. <https://doi.org/10.1016/j.neuroimage.2009.12.021>.
- Van Orden, G.C., Holden, J.G., Turvey, M.T., 2005. Human cognition and 1/f scaling. *J. Exp. Psychol. Gen.* 134 (1), 117–123. <https://doi.org/10.1037/0096-3445.134.1.117>.
- Vanneste, S., De Ridder, D., 2012. The auditory and non-auditory brain areas involved in tinnitus. An emergent property of multiple parallel overlapping subnetworks. *Front. Syst. Neurosci.* 6, 31. <https://doi.org/10.3389/fnsys.2012.00031>.

16 Log-dynamics in phantom sounds

- Vanneste, S., De Ridder, D., 2016. Deafferentation-based pathophysiological differences in phantom sound: tinnitus with and without hearing loss. *Neuroimage* 129, 80–94. <https://doi.org/10.1016/j.neuroimage.2015.12.002>.
- Vanneste, S., van de Heyning, P., De Ridder, D., 2011. The neural network of phantom sound changes over time: a comparison between recent-onset and chronic tinnitus patients. *Eur. J. Neurosci.* 34 (5), 718–731. <https://doi.org/10.1111/j.1460-9568.2011.07793.x>.
- Vanneste, S., Song, J.J., De Ridder, D., 2013. Tinnitus and musical hallucinosis: the same but more. *Neuroimage* 82C, 373–383. <https://doi.org/10.1016/j.neuroimage.2013.05.107>. S1053-8119(13)00610-1 [pii].
- Vanneste, S., Song, J.J., De Ridder, D., 2018. Thalamocortical dysrhythmia detected by machine learning. *Nat. Commun.* 9 (1), 1103. <https://doi.org/10.1038/s41467-018-02820-0>.
- Vanneste, S., Alsalman, O., De Ridder, D., 2019. Top-down and bottom-up regulated auditory phantom perception. *J. Neurosci.* 39 (2), 364–378. <https://doi.org/10.1523/JNEUROSCI.0966-18.2018>.
- Voytek, B., Knight, R.T., 2015. Dynamic network communication as a unifying neural basis for cognition, development, aging, and disease. *Biol. Psychiatry* 77 (12), 1089–1097. <https://doi.org/10.1016/j.biopsych.2015.04.016>.
- Voytek, B., Kramer, M.A., Case, J., Lepage, K.Q., Tempesta, Z.R., Knight, R.T., Gazzaley, A., 2015. Age-related changes in 1/f neural electrophysiological noise. *J. Neurosci.* 35 (38), 13257–13265. <https://doi.org/10.1523/JNEUROSCI.2332-14.2015>.
- Vysata, O., Prochazka, A., Mares, J., Rusina, R., Pazdera, L., Valis, M., Kukal, J., 2014. Change in the characteristics of EEG color noise in Alzheimer's disease. *Clin. EEG Neurosci.* 45 (3), 147–151. <https://doi.org/10.1177/1550059413491558>.
- Weinger, P.M., Zemon, V., Soorya, L., Gordon, J., 2014. Low-contrast response deficits and increased neural noise in children with autism spectrum disorder. *Neuropsychologia* 63, 10–18. <https://doi.org/10.1016/j.neuropsychologia.2014.07.031>.
- Yu, Y., Romero, R., Lee, T.S., 2005. Preference of sensory neural coding for 1/f signals. *Phys. Rev. Lett.* 94 (10), 108103. Retrieved from <http://www.ncbi.nlm.nih.gov/pubmed/15783530>.